Mon. Not. R. Astron. Soc. **397,** 325–334 (2009) doi:10.1111/j.1365-2966.2009.14906.x

Detection of non-radial pulsation and faint companion in the symbiotic star CH Cyg

E. Pedretti,[1★†] J. D. Monnier,[2] S. Lacour,[3] W. A. Traub,[4] W. C. Danchi,[5] P. G. Tuthill,[6] N. D. Thureau,[1] R. Millan-Gabet,[7] J.-P. Berger,[3] M. G. Lacasse,[8] P. A. Schuller[9] F. P. Schloerb[10] and N. P. Carleton[8]

[1]*School of Physics and Astronomy, University of St Andrews, North Haugh, St Andrews KY16 9SS*
[2]*University of Michigan, Astronomy department, 914 Dennison bldg., 500 Church street, Ann Arbor, MI 40109, USA*
[3]*Laboratoire d'Astrophysique de l'Observatoire de Grenoble (LAOG), 414 rue de la Piscine, BP 53-X Grenoble, France*
[4]*Jet Propulsion Laboratory, California Institute of Technology, M/S 301–451, 4800 Oak Grove Drive, Pasadena, CA 91109, USA*
[5]*NASA Goddard Space Flight Center, 8800, Greenbelt Road, Greenbelt, MD 20771, USA*
[6]*School of Physics, Sydney University, NSW 2006, Sydney, Australia*
[7]*Michelson Science Center, California Institute of Technology, 770 S. Wilson Ave. MS 100-22, Pasadena, CA 91125, USA*
[8]*Harvard–Smithsonian Center for Astrophysics, 60 Garden Street, Cambridge, MA 02138, USA*
[9]*Institut d'Astrophysique Spatiale, Universit Paris–Sud, bâtiment 121, 91405 Orsay Cedex, France*
[10]*University of Massachusetts, Astronomy Department, Amherst, MA 01003-4610, USA*

Accepted 2009 April 14. Received 2009 April 14; in original form 2009 February 8

ABSTRACT

We have detected asymmetry in the symbiotic star CH Cyg through the measurement of precision closure phase with the Integrated Optics Near-Infrared Camera (IONIC) beam combiner, at the infrared optical telescope array interferometer. The position of the asymmetry changes with time and is correlated with the phase of the 2.1-year period found in the radial velocity measurements for this star. We can model the time-dependent asymmetry either as the orbit of a low-mass companion around the M giant or as an asymmetric, 20 per cent change in brightness across the M giant. We do not detect a change in the size of the star during a 3-year monitoring period neither with respect to time nor with respect to wavelength. We find a spherical dust shell with an emission size of $2.2 \pm 0.1\ D_*$ full width at half-maximum around the M giant star. The star to dust flux ratio is estimated to be 11.63 ± 0.3. While the most likely explanation for the 20 per cent change in brightness is non-radial pulsation, we argue that a low-mass companion in close orbit could be the physical cause of the pulsation. The combined effect of pulsation and low-mass companion could explain the behaviour revealed by the radial velocity curves and the time-dependent asymmetry detected in the closure-phase data. If CH Cyg is a typical long secondary period variable then these variations could be explained by the effect of an orbiting low-mass companion on the primary star.

Key words: techniques: high angular resolution – techniques: interferometric – binaries: symbiotic – stars: imaging – stars: individual: CH Cygni.

1 INTRODUCTION

Symbiotic stars are objects presenting combination spectra of a hot ionized nebula and the cool continuum absorption molecular features of a late-type star. Nowadays, symbiotic stars are understood as mass-transfer binaries of short period, from a few to 10 years. The separation can vary from a few au to slightly more than 10 au. The symbiotic pair is usually composed of a cool giant star with an accreting compact object, either a white dwarf or a neutron star.

CH Cyg is one of the most studied of symbiotic variables. The star presents a composite spectrum of a M6-7 giant star during quiescent phase and a hot component blue continuum from 6000 to 9000 K temperature and low excitation line spectrum during the active phase (Deutsch et al. 1974). Webster & Allen (1975) classified the star as an S-type symbiotic with no hot dust, but long term multiwavelength photometry study of the star (Taranova & Iudin 1988) has shown that hot dust appeared in the system after the 1984 outburst. The dust was modelled as a spherical shell of inner

★Affiliated to Scottish universities physics alliance (SUPA).
†E-mail: ep41@st-and.ac.uk

© 2009 The Authors. Journal compilation © 2009 RAS

Downloaded from http://mnras.oxfordjournals.org/ at NASA Goddard Space Flight Ctr on July 1, 2014

radius of 15 au by Bogdanov & Taranova (2001) through spectral energy distribution fitting.

Dyck, van Belle & Thompson (1998) measured an angular diameter of 10.4 mas at 2.2 μm for CH Cyg with infrared interferometry. Young et al. (2000) observed CH Cyg with the Cambridge optical aperture synthesis telescope (COAST) in 1999. The obtained visibility and closure-phase data were best modelled by an elliptical, limb-darkened star. Their interpretation of these findings was that the ellipticity of the star was either due to an extension of the M giant atmosphere or due to the partial eclipse of an orbiting red giant companion as proposed by Skopal et al. (1996).

CH Cyg shows photometric and radial velocity variations. In photometry, two main periods are found: a small amplitude (0.1 mag), ∼100-d period (Mikolajewski, Mikolajewska & Khudyakova 1992) likely caused by stellar pulsation and a ∼770-d period (Mikolajewski et al. 1992) or a ∼1 mag, ∼750-d period (Skopal et al. 2007). These photometric variations are not always detected (Munari et al. 1996) and are not related to the 100-d pulsation period. Hinkle et al. (1993) pointed out that the photometric variations of CH Cyg are far longer than the fundamental pulsation mode for this star, which is a first-overtone pulsator (Mikolajewski et al. 1992). The radial velocity variations from the literature (Hinkle et al. 1993) show two periods: a 15.6-year long period and a 2.1-year (750-d) short period.

Hinkle et al. (1993) and Hinkle, Fekel & Joyce (2009) suggested a correlation between the 750/770-d photometric period and the 750-d radial velocity period. They also remarked that the photometric variations of CH Cyg are similar to those found in long secondary period (LSP) variable stars (Hinkle et al. 2006). This type of variability is found in some semiregular variables and in about the 25 per cent of the Large Magellanic Cloud (LMC) semiregular variables. Hinkle et al. (2002) and Wood, Olivier & Kawaler (2004) found that several semiregular variables also show spectroscopic behaviour consistent with LSP variability. The cause of the LSP is currently unknown but possible explanations are highlighted in Wood et al. (2004). They conclude that the most likely explanation for LSP variations is a low-order non-radial pulsation on the outer radiative layers of the giant star.

Wood et al. (1999) also discovered that LSP variables follow a period–luminosity (PL) relation which he called 'sequence D'. Soszynski et al. (2004) noted that Wood sequence-D variables overlap with sequence-E contact binaries, implying that sequence D is indeed a class of binaries. Soszyński (2007) also found that 5 per cent of LSPs in the LMC present ellipsoidal-like or eclipsing-like modulation that are usually shifted in phase with respect to LSP light curves.

Hinkle et al. (1993) proposed a model where CH Cyg was a triple system with the symbiotic pair in a 2.1-year orbit. The reasons for having the symbiotic pair on the 2.1-year orbit were that no known S-type symbiotic star had orbital period larger than 5 years, the 2.1-year period was too long for a M giant fundamental-mode pulsation and there was weak evidence for a high-inclination 15.6-year orbit. The third star was either regarded as a G–K dwarf (Hinkle et al. 1993) or an M giant (Skopal et al. 1996). The inclination of the 15.6-year orbit was unknown at the time but was recently inferred from the several eclipses reported in the literature (Mikolajewski, Mikolajewska & Tomov 1987; Eyres et al. 2002; Sokoloski & Kenyon 2003). Schmidt et al. (2006) suggested that the 2.1-year period was caused by a pulsation in the M giant and not by a close binary.

There is controversy on the shape of the possible orbit of the close pair. Hinkle et al. (1993) argued that the asymmetric line profiles could be caused by a M giant star irradiated by a white dwarf. An asymmetric line profile could lead to a false elliptic solution for an orbit obtained from radial velocities. According to Hinkle et al. (1993), the orbit of CH Cyg should be circular due to tidal interaction with the M giant.

Hinkle et al. (2009) re-examined the conclusions of the Hinkle et al. (1993) paper. They concluded that the 2.1-year velocity variation is consistent with LSP variation and that the white dwarf responsible for the activity in the system is on the 15.6-year orbit. The 2.1-year period would be caused either by non-radial pulsation of the star or by a low-mass companion in close orbit to the M giant.

This paper presents the results of infrared interferometric observations performed in 2004–2006 at the infrared optical telescope array (IOTA; Traub et al. 2004) and at the Keck-1 telescope fitted with an aperture mask. The main aim of this paper is to provide unique observational data that could help to understand the nature of the mysterious 2.1-year oscillation in radial velocity for this star.

2 OBSERVATIONS AND DATA REDUCTION

Observations were performed at the IOTA interferometer and at the Keck-1 telescope. IOTA was a long-baseline optical interferometer located at the Smithsonian Institution's Whipple Observatory on Mount Hopkins, AZ. IOTA operated from 1995 to 2006, and was used as a testbed for new cutting-edge technologies (Berger et al. 2001; Monnier et al. 2003). IOTA produced a large number of astronomy results over the past few years (Mennesson et al. 2002; Ohnaka et al. 2003; Monnier et al. 2004; Perrin et al. 2004; Kraus et al. 2005; Millan-Gabet et al. 2006; Monnier et al. 2006; Kraus et al. 2007; Zhao et al. 2007; Lacour et al. 2008; Ragland et al. 2008).

Observations performed at the Keck-1 telescope used the near-infrared camera (NIRC) and an aperture mask that converted the telescope pupil into a sparse interferometric array of 9.8 m maximum baseline. For detailed discussion of the Keck aperture-mask experiment and scientific rationale see Tuthill et al. (2000).

In Table 1, we present a journal of our observations, listing date, filter and calibrator star. In Table 2, we detail the physical properties of the calibrators. Our H-band data used the IONIC combiner (Berger et al. 2003) with narrow H-band filters at the IOTA interferometer and at the Keck telescope for the observations of 2004, while data were acquired using a standard H-band filter at IOTA for 2005. Data from 2006 used a low-dispersion spectrograph which provided seven spectral channels across the H-band with an $R = 39$. For a description of the spectrograph, see Ragland et al. (2003) and Pedretti et al. (2008). First results with the spectrograph were published by Lacour et al. (2008).

For the aperture-masking experiment, we refer the readers to the work of Monnier (1999) and Tuthill et al. (2000) for the data analysis, procedures adopted to extract visibilities and closure-phases in OIFITS format (Pauls et al. 2005).

The data reduction pipeline for the IONIC combiner was described in detail in Monnier et al. (2004). Briefly, the reduction of the squared visibilities (V^2) followed the same method explained by Coude Du Foresto, Ridgway & Mariotti (1997). Interferograms were corrected for intensity fluctuations and bias terms from readout noise and photon noise. The power spectrum of each interferogram was calculated in order to measure V^2. A transfer matrix was used to take in account the variable flux ratio for each baseline. The absolute calibration accuracy was studied by Monnier et al. (2004) by observing single stars of known size.

Downloaded from http://mnras.oxfordjournals.org/ at NASA Goddard Space Flight Ctr on July 1, 2014

Table 1. Log of observations. The IOTA 3T telescope configuration refers to the location of the A, B, C telescopes along the NE, SE and NE arms.

Date (UT)	Mean JD	Phase	Telescope	λ (μm)	Δλ (μm)	R^a	Calibrator names
2004 April 23	245 3119	0.40	IOTA, A35-B15-C10	1.51	0.090		α Lyr, α Aql
2004 April 24	245 3120	0.40	IOTA, A35-B15-C10	1.64	0.100		α Lyr, α Aql
2004 April 25	245 3121	0.40	IOTA, A35-B15-C10	1.64	0.100		α Lyr, α Aql
2004 April 26	245 3122	0.40	IOTA, A35-B15-C10	1.78	0.090		α Lyr, α Aql
2004 April 29	245 3125	0.41	IOTA, A35-B15-C10	1.78	0.090		α Lyr, ρ Ser
2004 April 30	245 3126	0.41	IOTA, A35-B15-C10	1.78	0.090		α Lyr, ν Hya
2004 May 01	245 3127	0.41	IOTA, A35-B15-C10	1.78	0.090		α Lyr, α Aql
2004 September 04	245 3105	0.38	Keck A, Golay mask	1.64	0.025		α Lyr
2005 June 06	245 3528	0.94	IOTA, A35-B15-C10	1.66	0.300		α Lyr
2005 June 08	245 3530	0.95	IOTA, A25-B15-C10	1.66	0.300		α Lyr
2006 April 24	245 3850	0.37	IOTA, A35-B15-C10	1.66	0.300	39	α Lyr, βHer
2006 April 30	245 3856	0.38	IOTA, A35-B15-C10	1.66	0.300	39	α Lyr, βHer
2006 May 01	245 3857	0.38	IOTA, A35-B15-C10	1.66	0.300	39	α Lyr, βHer
2006 May 02	245 3858	0.38	IOTA, A35-B15-C10	1.66	0.300	39	α Lyr, βHer

[a]Only applicable to the IOTA spectrograph.

Table 2. Calibrator information.

Calibrator name	Spectral type	Adopted UD (mas)	Reference(s)
α Lyr	A0V	3.22 ± 0.01	Absil et al. (2006)
β Her	G7IIIa	3.40 ± 0.03	This work
ρ Ser	K5III	3.28 ± 0.04	Bordé et al. (2002)
α Aql	A7V	3.46 ± 0.04	van Belle et al. (2001)

Closure phases for the IONIC combiner were obtained using two independent methods: one was developed by Baldwin et al. (1996) for the COAST and the other by Hale et al. (2003) for the infrared spatial interferometer. In order to measure meaningful closure phase, fringes must at least be present in three baselines and the fringe packets must overlap, to be detected in the same coherence time. The largest error in closure-phase offset for a point source was caused by chromaticity in the combiner which limits the absolute precision when source and calibrator are not of the same spectral type. Engineering tests performed by Monnier et al. (2004) showed that the closure phase varied systematically by $1.4 \pm 0\overset{\circ}{.}3$ between a cool star of spectral type M3 and a hot B8 star.

The IOTA data pipeline produced visibility and closure phases in OIFITS format, which can be easily imported in imaging or modelling programmes using libraries provided by John Young, for C and PYTHON[1] and John Monnier for IMAGE DATA LANGUAGE (IDL).[2] A standard 2 per cent systematic error was added in quadrature to the visibility and closure-phase data as in Monnier et al. (2004). Calibrated data in OIFITS format will be made available on request for interested investigators.

3 MODELLING

Wood et al. (2004) conducted a thorough review on the causes of the LSP variations in asymptotic giant branch (AGB) stars. They ruled out several possible models, among which were radial pulsation, companion in close orbit, spots on the star and modulation from an ellipsoidal-shaped AGB star. They concluded that non-radial pulsation was the most likely explanation for LSP. In their recent paper, Hinkle et al. (2009) after a thorough review of the literature on CH Cyg applied a similar approach to rule out possible models explaining the 2.1-year change in radial velocity in CH Cyg. We used our interferometry data to verify some of the hypotheses discussed in these papers. Due to limited uv-plane coverage of the data (see Fig. 1), in particular for the 2005 epoch, we could not resort to model-independent imaging of the CH Cyg system. For this reason, we used parametric modelling to derive the size of the star, the full width at half-maximum (FWHM) size of the dust and the position and distance of the asymmetries detected in the closure-phase data. For model fitting, we used publicly available least-squares minimization routines.[3]

Our modelling was similar to Ragland et al. (2008) except that we did not need to model multiwavelength sizes for the star, since CH Cyg does not change size appreciably with respect to wavelength. We decided to test the following hypothesis to investigate the cause of the LSP variations and to interpret our data: (1) radial pulsation of the star; (2) presence of dust inside the 15.6-year orbit (3) spots on the star; (4) M giant companion in a 15.6-year orbit; (5) dwarf companion in a 2.1-year orbit; (6) non-radial pulsation.

3.1 Radial pulsation and dust

In order to test (1) and (2), a simple model composed of a uniform disc (UD) for the star and a Gaussian disc (GD) for the dust was first attempted in order to obtain a size for the star and for the dust. All data from all epochs were used for this model since, by visual inspection, our visibility points superposed quite well, indicating that the size of the star did not change appreciably outside the error bars of the data, neither with time nor with wavelength or position angle.

Fig. 2 shows the result of the fit. The data were smoothed using an azimuthal average due to the otherwise very large number of data points present on the graph. For each bin, we used the mean of the original data points weighted by their errors. The error on each new data point was the standard deviation for the bin. The

[1] http://www.mrao.cam.ac.uk/research/OAS/oi_data/oifits.html
[2] http://www.astro.lsa.umich.edu/monnier/oi_data/index.html
[3] A non-linear least-squares curve fitting (MPFIT), developed by Craig Marquardt. http://cow.physics.wisc.edu/craigm/idl/.

Downloaded from http://mnras.oxfordjournals.org/ at NASA Goddard Space Flight Ctr on July 1, 2014

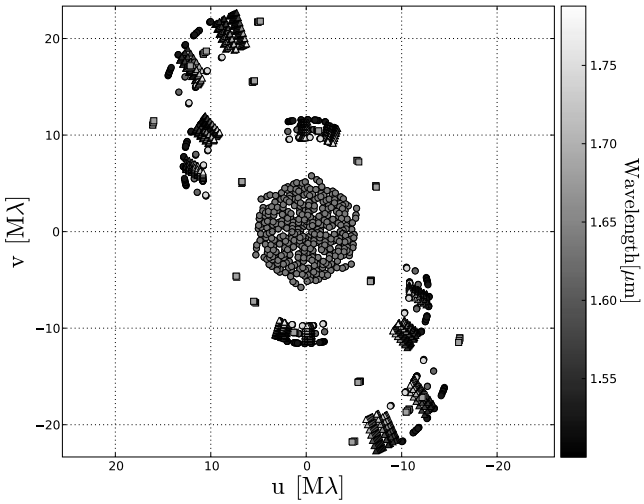

Figure 1. The *uv* coverage for CH Cyg for 2004 (circles) 2005 (squares) and 2006 (triangles). The shades of grey represent the wavelength of the data points.

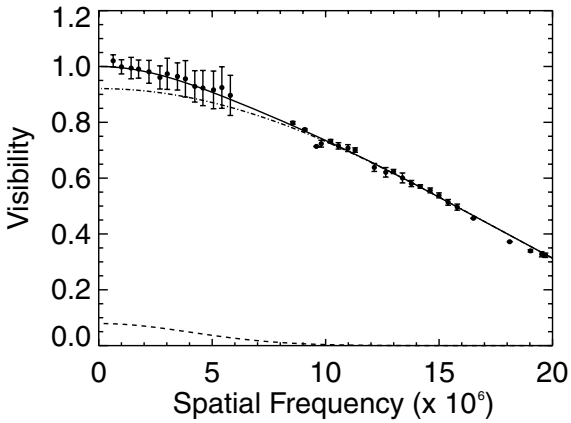

Figure 2. Visibility plot comprising all data from 2004 to 2006. A simple UD plus a GD model representing the star and the dust are superposed to the data. The contributions from the dust (dashed line) and the star (dash–dotted line) are also overplotted for clarity.

fit was performed on the original and non-smoothed data. Table 3 shows the parameters obtained from the fit. The value of 8.74 ± 0.02 for the diameter of the M giant is the most accurate so far thanks to the large amount of data used. This value is close to the value of 7.8 ± 0.6 obtained with infrared interferometry in 2001 June by Hofmann et al. (2003) using a simple UD fit. The errors were derived using bootstrap statistics on the data set. The FWHM size of the Gaussian dust emission was 19.13 ± 1.00 mas or 2.2 ± 0.1 stellar diameters FWHM, showing that hot dust exists close to the M giant. A marginally improved reduced χ^2 was obtained by fitting an elliptical dust distribution around the star. However, the difference in reduced χ^2 was too small in order to justify an asymmetric model for the dust emission in the near-infrared. The parameters from the elliptical dust-emission model are also listed in Table 3.

Thompson, Creech-Eakman & van Belle (2002) monitored an oxygen-rich and a carbon-rich Mira star measuring the change of angular size with respect to the pulsation cycle at the Palomar testbed interferometer. We did not detect any such change in CH Cyg. Unfortunately, our coverage of the 2.1-year period was quite limited (basically, two points at phase 0.4 and one point at phase 0.9 of the 'orbital' period). This coverage is insufficient to completely rule out radial pulsation for this star. However, we note that Hofmann et al. (2003) obtained a diameter of 7.8 ± 0.6 mas in 2001 June, using a simple UD model with three visibility points. Considering the crude UD model used that does not take into consideration the dust shell, this diameter is not very different from our measurement and would indicate that the star did not change diameter with time. Also, radial pulsation was ruled out by Hinkle et al. (2009) as the cause for secondary period in CH Cyg since the PL relation for AGB stars (Hughes & Wood 1990) would produce a period of about 250 d for a $K = -7.5$ star not 770 d.

3.2 Spots on the star

In order to model the closure-phase signal expected from a spotted star, we used an additional UD that could be placed at different position angles and separation from the centre of the UD + GD model representing the M giant and the dust emission. Flux ratios between

Table 3. Size of star and size of the dust-shell emission.

Size M giant (mas)	FWHM dust[a] (mas)	Flux ratio (M giant /dust)	PA (°)	Axis ratio dust (M/m)	Reduced χ^2
8.74 ± 0.02	19.1 ± 1.0	11.6 ± 0.3	0.0	1.0	1.3
8.74 ± 0.02	19.2 ± 0.9	11.6 ± 0.1	103 ± 5	1.28 ± 0.01	1.2

Note. We used a UD to model the star and a GD to model the dust. A model with a spherical dust-emission and a model with an elliptical dust-emission were attempted. The two models produced a very similar reduced χ^2.
[a]Size of the dust emission.

Downloaded from http://mnras.oxfordjournals.org/ at NASA Goddard Space Flight Ctr on July 1, 2014

the M giant and the companion/spot and between the M giant and the dust were allowed to change. The size of the additional UD was also free to change. The three epochs were analysed separately in order to detect asymmetries that would change with the observing epoch. We performed a parameter-space search in an attempt to identify the position of the asymmetry.

We could not find any solution with an unresolved or moderately resolved spot on the surface of the star. All the solutions converged to structure outside the disc of the M giant unless we restricted the flux to 10 per cent or more of the flux of the M giant as done in Section 3.3.

3.3 M giant companion on the 15.6-year orbit

We tested the hypothesis that the companion is a red giant in the 15.6-year orbit as discussed in the model proposed by Skopal et al. (1996). That model was devised to explain the eclipses observed in the 15.6-year orbit and kept the symbiotic pair in the 2.1-year orbit, given that there are no known symbiotic stars found on an orbit of period as long as 15.6 years. We restricted the flux ratio of the M giant/companion to values around 8.6, as expected in Taranova & Shenavrin (2004). The field of view (FOV) of IOTA was limited by the bandwidth of the photometric filter used: $\mathrm{FOV} = \lambda^2/\Delta\lambda B$, where λ is the wavelength, $\Delta\lambda$ is the bandwidth and B is the baseline. For the largest bandwidth used (0.3 μm at 1.65 μm) and a baseline of 38 m we obtained a minimum FOV of 50 mas. We performed a 50-mas wide search in all our data sets.

We did not find any trace of a companion in our best data sets of 2004 and 2006 when using the Taranova flux ratio. A second red giant should have been evident in the data. In particular, the Keck telescope aperture-masking experiment should have easily detected a second giant star down to a flux ratio M giant/companion of about 100 (Ireland et al. 2008; Kraus et al. 2008).

3.4 Dwarf companion in a 2.1-year orbit

We tested the hypothesis of a faint companion orbiting the M giant as in Sections 3.2 and 3.3. We restricted the flux contribution of the companion to less than 2 per cent of the total flux in order to simulate a large Δm between the M giant and the companion. As a consequence, we found asymmetries outside the M star in all three data sets. Fig. 3 shows the likelihood maps obtained from the reduced χ^2 surfaces. The dotted line ellipses are the errors on the positions of the companion which are quite large in the east–west direction due to the limited *uv* coverage of the IOTA in that direction.

Table 4 lists the separations, position angles, flux ratios and reduced χ^2 of the asymmetries for the three epochs. The UD size of the companion converged to a point source for all epochs. The error bars on the parameters were derived from the error ellipses. The 2005 data set converged to two separate solutions: one at 8-mas separation and another 32-mas separation. The second solution was likely due to a degeneracy caused by the limited amount of data available for the 2005 epoch. We could fit the 2.1-year elliptical orbit to the 32-mas position, with a χ^2 of 0.3. The semimajor axis of this orbit was 25.6 ± 0.8 mas which produced a far smaller luminosity and a much shorter distance than expected for this star. For this reason, we excluded this solution. We must point out that Balega et al. (2007) detected a faint companion with speckle interferometry in 2004 at 43 ± 1 mas separation and $24\overset{\circ}{.}1 \pm 2\overset{\circ}{.}1$ position angle. However, we do not believe that our 32-mas position is related to this detection. In fact, the Keck telescope aperture-masking experiment should have easily detected a companion down to a flux ratio M giant/companion of about 100 in our 2004 data (Ireland et al. 2008; Kraus et al. 2008), but such detection did not happen.

In order to investigate the hypotheses that the detected asymmetries were the signature of a faint companion in a 2.1-year orbit, we attempted orbit fits to the astrometric positions derived from the IOTA closure-phase data using infrared radial velocity orbital solutions from Hinkle et al. (2009). We attempted orbital fits using a circular orbit (Fekel, personal communication) which was discarded in Hinkle et al. (2009) due to the large residuals in the orbit fit. We also used the elliptical orbit solution from Hinkle et al. (2009). We obtained a reduced χ^2 of 0.1 for the circular orbit and a reduced χ^2 of 0.3 for the elliptical orbit. Such small reduced χ^2 values are possible given the small number of degrees of freedom (3 from the six data points and three free parameters) and the quite large error bars on the astrometric positions. The obtained orbits are shown in Fig. 4. The combined orbital parameters from radial velocity and interferometry and some derived parameters are shown in Table 5. The first part of the table lists the orbital parameters from Hinkle et al. (2009) and Fekel (personal communication). The errors on the parameters obtained from interferometry were derived using Monte Carlo simulations.

3.5 Non-radial pulsation

Although we could not obtain acceptable reduced χ^2 from the 'spots on the star' model, we managed to obtain reasonably good fits in simulations of large asymmetries on the star. We used low-order spherical harmonics to simulate large flux variations (up to 20 per cent) across the star. Such a dramatic brightness change could simulate the closure-phase signal of CH Cyg but seemed an unlikely explanation even in term of non-radial pulsation: we are not aware of any physical mechanism that could produce such a dramatic change of brightness across a star. Fig. 5 shows the models and the corresponding fits of visibility and closure phase. The reduced χ^2 was reasonably close to the dwarf-companion model. The asymmetry appears to rotate with the 2.1-year period.

4 DISCUSSION

Hinkle et al. (2009) restricted the possible explanation for the 2.1-year secondary period of CH Cyg to a low-order g-mode non-radial pulsation of the M giant or to a low-mass companion (0.2 $M_\odot$) in close orbit to the M giant. In this model, the companion responsible for the activity is on the 15.6-year orbit.

According to Hinkle et al. (2009), a 0.2 $M_\odot$ companion would have a temperature of about 3200 K and would be spectroscopically indistinguishable from the M giant. Since CH Cyg is single-lined binary/triple star, the masses of the components cannot be derived directly. We can, however, test the derived parameters against the published literature, assuming the mass of one of the components. Table 6 shows the change of the derived parameters for different values of the mass of the companion. M_1 is the mass of the M giant in solar masses, R_1 is the radius in solar radii, L_1 is the luminosity in solar luminosities. The semimajor axis '*a*' of the orbit in physical units of au was obtained using Kepler's law. D is the distance in parsecs. The table is divided in two parts, one concerned with the circular orbital solution and one with the elliptical solution.

The mass of 2 $M_\odot$ from Hinkle et al. (2009), a luminosity of 6900 $L_\odot$ from Biller et al. (2006) and a radius of 280 ± 65 $R_\odot$ obtained by Schild et al. (1999) through infrared spectroscopy were used to restrict the solutions listed in Table 6. A value of 0.32 $M_\odot$

Downloaded from http://mnras.oxfordjournals.org/ at NASA Goddard Space Flight Ctr on July 1, 2014

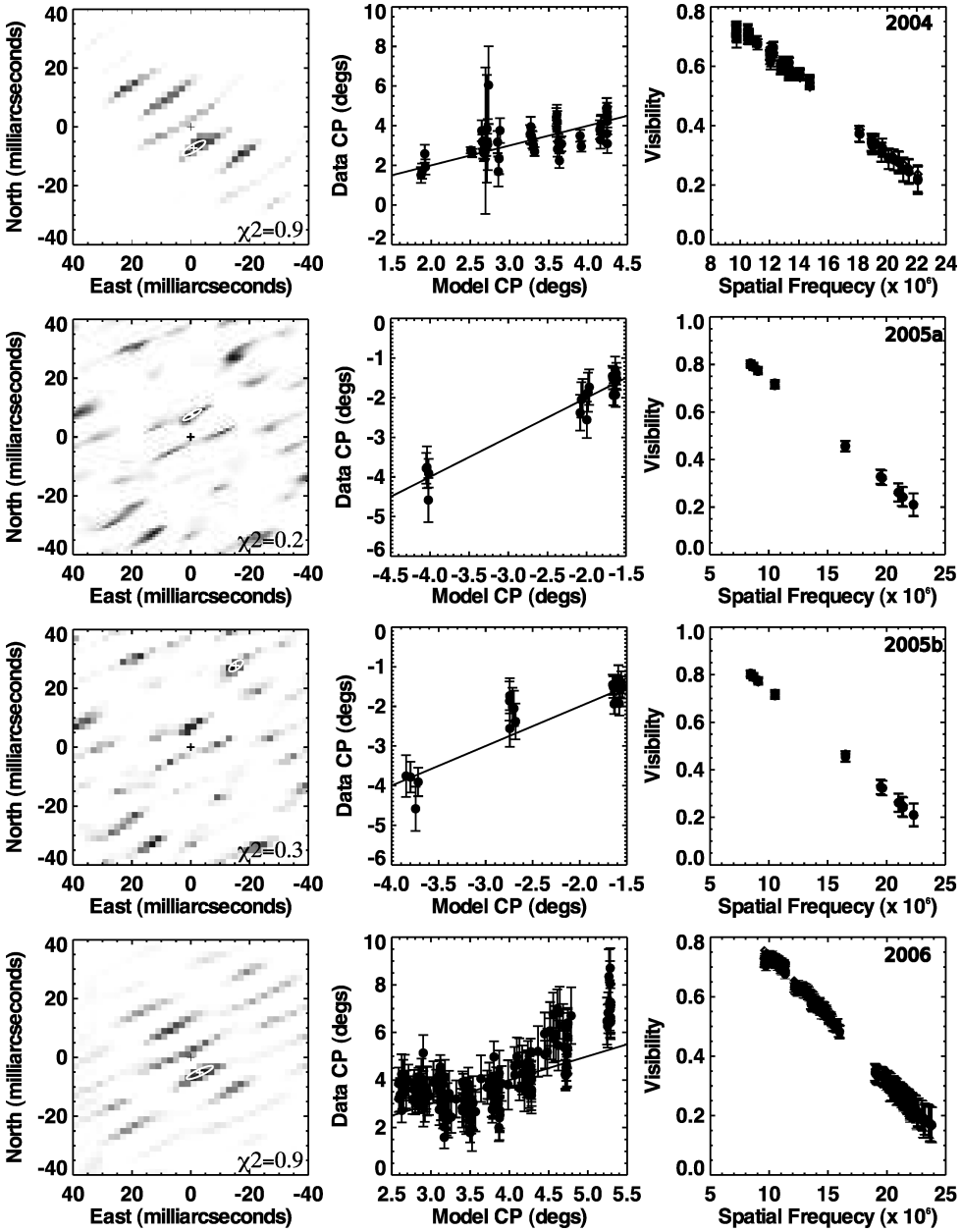

Figure 3. Binary–star search in χ^2 space. A simple binary–star model was fitted to the visibility and closure-phase data from different epochs. The M giant was kept at the centre of the field while the companion was placed in all possible positions of a 40 × 40 mas^2 grid. A reduced χ^2 value was obtained for each position and the values recorded on a two-dimensional array. Left-hand column shows a likelihood surfaces derived from the χ^2 arrays for our 2004, 2005a and 2005b (non-unique solutions) and 2006 data. The positions of the asymmetries are encoded in the likelihood map. The white crosses represent the positions of the asymmetry and the white ellipses encode the uncertainty of the position. The centre column shows data-versus-model plots for closure phase. Right-hand column shows visibility-versus-spatial-frequency plots (filled circles) with superposed points derived from the model (open diamonds). Note that the high density of data points makes it very hard to distinguish between filled circles and open diamonds. We observed that the closure phase flipped sign between 2004 and 2005 and between 2005 and 2006 meaning that the detected asymmetry was in the opposite direction in 2005.

for the low-mass companion yielded a mass of 2 $M_\odot$, a radius of 250 $R_\odot$ and a luminosity of 6517 $L_\odot$ for the M giant, very close to the values from the literature.

Also, the distance obtained from the size of the circular orbit derived using Kepler's law and the apparent size of the orbit in milliarcseconds was 296 pc, comparable within errors to the 244^{+49}_{-35} pc distance obtained from the revisited data reduction of the *Hipparcos* parallax (van Leeuwen 2007).

Soszynski et al. (2004) found that Wood's sequence-D variables are a continuation of sequence-E ellipsoidal variables. Soszynski et al. (2007) require that the ratio between the radius of the star and the semimajor axis of the orbit should be $R/a \sim 0.4$ for the binary explanation of the LSP [equation 5 in Soszynski et al. (2007)]. For our circular orbit solution, the ratio derived by the angular diameter of the star and the semimajor axis of the hypothetical orbit is 0.6, ∼50 per cent larger than the required value.

Soszyński (2007) also proposed a model where the LSP variation are caused by mass loss from the giant to the low-mass companion. Since we detected hot-dust emission inside the possible 2.1-year orbit, we cannot exclude that LSP photometric variation are caused

Downloaded from http://mnras.oxfordjournals.org/ at NASA Goddard Space Flight Ctr on July 1, 2014

Table 4. Orbital positions for the low-mass object.

Mean JD	Separation (mas)	PA (°)	Flux ratio M giant/ dwarf	Flux ratio M giant/ dust	Reduced χ^2
245 3122.9	7^{+3}_{-2}	188^{+37}_{-26}	78 ± 1	9.6 ± 0.4	0.9
245 3529.0	8^{+3}_{-2}	356^{+4}_{-4}	88 ± 5	18.7 ± 1.0	0.2
245 3529.0	32^{+3}_{-3}	331^{+3}_{-3}	104 ± 4	18.4 ± 0.8	0.3
245 3855.2	6^{+2}_{-1}	211^{+37}_{-42}	74 ± 1	14.2 ± 0.4	0.9

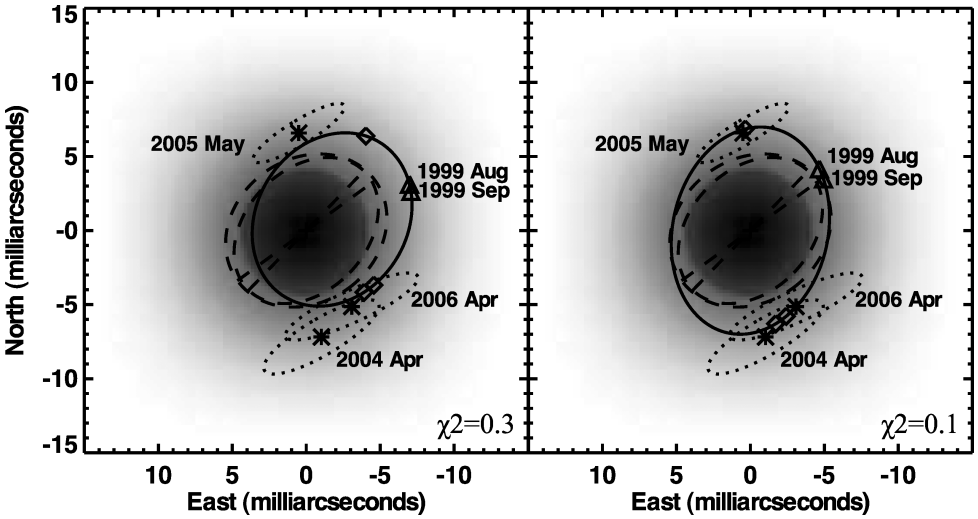

Figure 4. The astrometric orbit of CH Cyg. The plots show an elliptical orbit fit (left-hand panel) and a circular orbit fit (right-hand panel). Superposed to the orbits is a UD representing the star and a GD representing the dust emission in the system. The flux contribution from the dust was exaggerated to render the dust extent visible in the picture. The diamonds are the expected positions of the companion relative to the M giant, according to the ephemeris. The observed positions of the secondary component are marked with error ellipses (dotted line) centred around a star symbol. The triangles are the expected positions of the companion during the observations at the COAST interferometer. The dashed line ellipses represent an elliptical model of CH Cyg from Young et al. (2000). The major axis of the ellipses is also shown to better appreciate the orientation of the ellipses.

Table 5. Orbital parameters of the possible low-mass object.

Parameters	Circular solution	Elliptical solution
	Radial velocity	
P (d)	749.8 ± 2.3	750.1 ± 1.3
$T0$ (HJD)	2446 823.2 ± 7.7	2447 293.5 ± 12.9
ω (°)	0.0	229.5 ± 7.7
e	0.0	0.330 ± 0.041
K (Km s^{-1})	2.87 ± 0.13	2.87 ± 0.13
γ (Km s^{-1})	−59.93 ± 0.10	−59.91 ± 0.09
$a \sin\ i$ (Km)	$2.96 \times 10^7 \pm 0.29 \times 10^7$	$2.79 \times 10^7 \pm 1.23 \times 10^7$
$f(m)$ (M$_\odot$)	0.000 18 ± 0.0002	0.000 15 ± 0.0002
	Interferometry	
i (°)	138 ± 10	146 ± 6
Ω (°)	347 ± 7	337 ± 8
a (mas)	7.1 ± 0.3	6.3 ± 0.3

by dust trailing the low-mass companion. There have been claims of eclipses in the 2.1-year orbit of CH Cyg (Skopal et al. 1996; Iijima 1998). The inclination of the circular orbit obtained from the interferometric data would prevent eclipses but if the dust is clumpy and is trailing the companion it could be responsible for occasional photometric variations and could simulate eclipses.

Another clue in favour of the low-mass companion explanation for the LSP variation of CH Cyg comes from the independent interferometric observations of Young et al. (2000) at the wavelength of 905 nm. The visibility and closure-phase data from the COAST interferometer were modelled by an elliptical, limb-darkened star (parameters from that model are reproduced in Table 7). Fig. 4 shows the astrometric orbit of CH Cyg for the elliptical and circular orbit solution superposed to the models from Young et al. (2000). Interestingly, the minor axis of the two ellipses is very close to the radius of the M giant obtained from our model, while the major axis intersects the predicted orbital position of the companion on the circular orbit. The major axis of the ellipses did not intersect the orbital positions of the companion on the elliptical orbit. Also, our elliptical orbit fit to our astrometric positions had a χ^2 three-times worse than the circular orbit fit.

According to Hinkle et al. (2009), the most powerful argument against the close-binary explanation of LSP variation in CH Cyg is the shape of the radial velocity curve: the most likely orbit for the low-mass companion would be elliptical due to the large radial velocity residuals obtained from fitting a circular orbit. On the other hand, Hinkle et al. (2009) derived a mass of 2.0 M$_\odot$ for the M star, based on evolutionary arguments and argued that the Roche lobe for a 2–0.2 M$_\odot$ binary would constantly change from $(1 + e)a$ at apoastron to $(1 - e)a$ at periastron for an elliptical orbit. A 280 R$_\odot$ giant would fill the Roche lobe at each periastron passage generating

Downloaded from http://mnras.oxfordjournals.org/ at NASA Goddard Space Flight Ctr on July 1, 2014

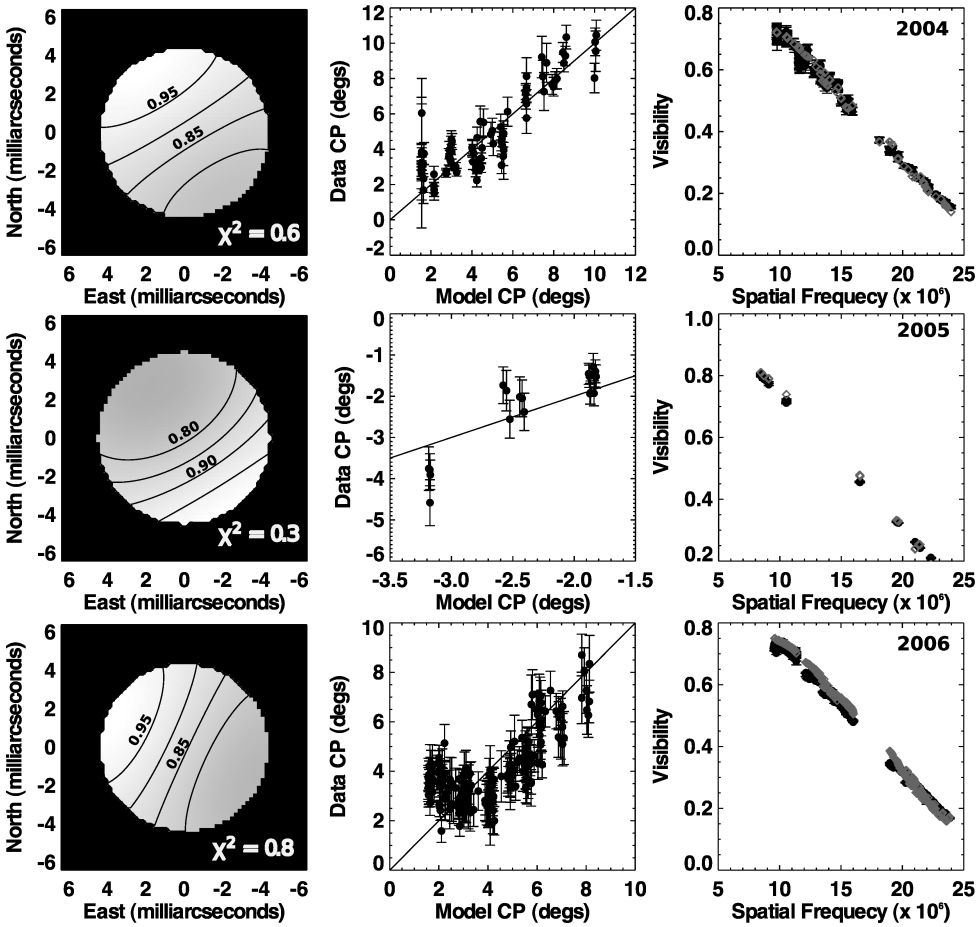

Figure 5. The 2004 to 2006 visibility and closure-phase data were also fit by an asymmetric brightness distribution on the surface of the star. The left-hand column shows models of the star for different epochs. The asymmetric flux distribution was modelled using spherical harmonics. The centre column shows data-versus-model plots for the closure phase. The right-hand column shows visibility-versus-spatial-frequency plots (filled circles) with superposed points derived from the model (open diamonds). The asymmetric change in brightness across the star could be caused by a non-radial pulsation (Wood et al. 2004; Hinkle et al. 2009). However, we are not aware of any pulsation mechanism that would produce a 20 per cent change in brightness across the star. The closure phase changed sign and the asymmetry flipped of 180° in 2005.

Table 6. Derived red giant parameters as a function of the faint companion's mass.

M_2 ($M_\odot$)	0.1	0.2	0.3	0.4	0.5	0.6
			Circular orbit			
M_1 ($M_\odot$)	0.3	0.9	1.8	2.8	3.9	5.2
R_1 ($R_\odot$)	156	221	270	312	349	382
L_1 ($L_\odot$)	2037	4073	6110	8146	10 183	12 219
a (au)	1.2	1.7	2.0	2.3	2.6	2.9
D (pc)	166	235	288	332	371	407
			Elliptical orbit			
M_1 ($M_\odot$)	0.2	0.7	1.4	2.2	3.2	4.2
R_1 ($R_\odot$)	165	233	285	330	369	404
L_1 ($L_\odot$)	2267	4534	6801	9068	11 335	13 601
a (au)	1.5	1.6	1.9	2.2	2.5	2.7
D (pc)	143	248	304	351	392	430

large mass loss. We argue that distortion by proximity effect (Eaton 2008) could also change the shape of the radial velocity curve and therefore the circular orbit solution cannot be eliminated on the basis of this argument.

Hinkle et al. (2009) argue that non-radial pulsation could also reproduce the observed radial velocities and photometric variation of CH Cyg. The problem with the non-radial pulsation argument is that low-order g modes are evanescent in convective regions and there is no known physical mechanism that could explain the non-radial pulsation for M giant stars where radiative transfer is mostly convective. As we show in Fig. 5, an asymmetric brightness distribution on the surface of the star could also reproduce our observed closure-phase signature. The flux variation across the star must be very large (20 per cent) in order to explain the closure-phase results and we are not aware of any physical mechanism that could produce such a dramatic change of brightness across a star.

Table 7. Elliptical star model parameters from Young et al. (2000).

Epoch	Major axis (mas)	Axial ratio	PA (°)
99/08	11.5 ± 0.2	0.84 ± 0.05	126 ± 9
99/09	11.2 ± 0.2	0.79 ± 0.03	136 ± 5

Close encounter with another object can produce non-radial oscillations on a fluid star through tides according to Eriguchi (1990). Circularization of early-type main-sequence binaries is also known to cause non-radial g-mode resonant oscillations. In late-type stars,

Downloaded from http://mnras.oxfordjournals.org/ at NASA Goddard Space Flight Ctr on July 1, 2014

turbulence is very efficient in damping these oscillation and circularizing binary orbits. Ivanov & Papaloizou (2004) studied tides in fully convective stars. They came to the conclusion that resonant tides may be possible in fully convective stars.

CH Cyg is a very complex object. If it is a triple system, the interactions of the companions with the M star could be very complex. The signature in the radial velocity could be caused by a combination of the movement of the low-mass companion and non-radial pulsation of the star. This could explain the residuals found in fitting a circular orbit to the radial velocity data. The non-radial pulsation may be due to tidal interaction of the low-mass companion with the M giant. Such interaction would also cause rapid circularization of the orbit for the low-mass companion.

It is not clear what the time-scale for the circularization of the orbit and the dissipation of the non-radial pulsation would be. If the dissipation of the non-radial pulsation by convective turbulence is efficient and the time-scale for circularization is short, it is hard to explain why at least 25 per cent of stars in globular clusters show LSP variations. We suggest that in globular clusters interactions with low-mass companions could be more frequent than expected. LSP variations then would be caused by non-radial pulsations excited by orbital capture of a companion or circularization of an elliptical orbit.

5 CONCLUSIONS

We have presented simple models in order to explain the asymmetries detected through infrared interferometry in the S-type symbiotic star CH Cyg. We do not detect significant change of angular size (8.74 ± 0.02 mas) for the M giant over a 3-year period, rendering radial pulsation a less likely explanation for the 2.1-year variability in radial velocity data. We find a spherical hot dust shell with an emission size of $2.2 \pm 0.1\ D_*$ FWHM around the M giant star which could be responsible for some of the reported short-period eclipses. We find correlation between the 2.1-year variability and the variation in our closure phase. We model the closure phase as a large change in brightness across the M giant and/or a low-mass companion in close orbit around the star. While the most likely explanation for the change in brightness can be a non-radial pulsation, we argue that a low-mass companion in close orbit could be the physical cause of the pulsation. The combined effect of pulsation and low-mass companion in close orbit to the M giant could explain the behaviour of the radial velocity curves and the asymmetries detected in the closure-phase data. If CH Cyg is a typical LSP variable then LSP variations could be explained by the effect of an orbiting low-mass companion on the primary star.

ACKNOWLEDGMENTS

We acknowledge Leslie Hebb for a useful discussion. We thank Kenneth Hinkle and Francis Fekel for making available to us their data and results prior to publication and for many useful discussions and advice. This research was made possible thanks to a Michelson Postdoctoral Fellowship and a SUPA advanced fellowship awarded to E. Pedretti. N. Thureau received research funding from the European Community's Sixth Framework Programme through an International Outgoing Marie-Curie fellowship OIF – 002990.
The IONIC project is a collaboration among the Laboratoire d'Astrophysique de Grenoble (LAOG), Laboratoire d'Electromagnetisme Microondes et Optoelectronique (LEMO), and also CEA-LETI and IMEP, Grenoble, France. The IONIC project is funded in France by the Centre National de Recherche Scientifique and Centre National d'Etudes Spatiales. This research has made use of NASA's Astrophysics Data System Bibliographic Services and of the SIMBAD. data base operated at CDS, Strasbourg, France.

REFERENCES

Absil O. et al., 2006, A&A, 452, 237
Baldwin J. E. et al., 1996, A&A, 306, L13
Balega I. I., Balega Y. Y., Maksimov A. F., Malogolovets E. V., Rastegaev D. A., Shkhagosheva Z. U., Weigelt G., 2007, Astrophys. Bull., 62, 339
Berger J. P. et al., 2001, A&A, 376, L31
Berger J.-P. et al., 2003, Proc. SPIE, 4838, 1099
Biller B. A. et al., 2006, ApJ, 647, 464
Bogdanov M. B., Taranova O. G., 2001, Astron. Rep., 45, 797
Bordé P., Coudé du Foresto V., Chagnon G., Perrin G., 2002, A&A, 393, 183
Coude Du Foresto V., Ridgway S., Mariotti J.-M., 1997, A&AS, 121, 379
Deutsch A. J., Lowen L., Morris S. C., Wallerstein G., 1974, PASP, 86, 233
Dyck H. M., van Belle G. T., Thompson R. R., 1998, AJ, 116, 981
Eaton J. A., 2008, ApJ, 681, 562
Eriguchi Y., 1990, A&A, 229, 457
Eyres S. P. S. et al., 2002, MNRAS, 335, 526
Hale D. D. S., Fitelson W., Monnier J. D., Weiner J., Townes C. H., 2003, Proc. SPIE, 4838, 387
Hinkle K. H., Fekel F. C., Johnson D. S., Scharlach W. W. G., 1993, AJ, 105, 1074
Hinkle K. H., Lebzelter T., Joyce R. R., Fekel F. C., 2002, AJ, 123, 1002
Hinkle K., Fekel F., Joyce R., Wood P., 2006, Mem. Soc. Astron. Ital., 77, 523
Hinkle K., Fekel F., Joyce R., 2009, ApJ, 692, 1360
Hofmann K.-H. et al., 2003, Proc. SPIE, 4838, 1043
Hughes S. M. G., Wood P. R., 1990, AJ, 99, 784
Iijima T., 1998, MNRAS, 297, 77
Ireland M. J., Kraus A., Martinache F., Lloyd J. P., Tuthill P. G., 2008, ApJ, 678, 463
Ivanov P. B., Papaloizou J. C. B., 2004, MNRAS, 353, 1161
Kraus S. et al., 2005, AJ, 130, 246
Kraus S. et al., 2007, A&A, 466, 649
Kraus A. L., Ireland M. J., Martinache F., Lloyd J. P., 2008, ApJ, 679, 762
Lacour S. et al., 2008, A&A, 485, 561
Mennesson B. et al., 2002, ApJ, 579, 446
Mikolajewski M., Mikolajewska J., Tomov T., 1987, Ap&SS, 131, 733
Mikolajewski M., Mikolajewska J., Khudyakova T. N., 1992, A&A, 254, 127
Millan-Gabet R. et al., 2006, ApJ, 645, L77
Monnier J. D., 1999, PhD thesis, Univ. of California at Berkeley
Monnier J. D., Berger J. P., Millan-Gabet R., Traub W. A., Carleton N. P., Pedretti E., Coldwell C. M., Papaliolios C. D., 2003, Proc. SPIE, 4838, 1127
Monnier J. D. et al., 2004, ApJ, 602, L57
Monnier J. D. et al., 2006, ApJ, 647, 444
Munari U., Yudin B. F., Kolotilov E. A., Tomov T. V., 1996, A&A, 311, 484
Ohnaka K. et al., 2003, A&A, 408, 553
Pauls T. A., Young J. S., Cotton W. D., Monnier J. D., 2005, PASP, 117, 1255
Pedretti E. et al., 2008, Proc. SPIE, 7013, 70132V-1
Perrin G., Ridgway S. T., Coudé du Foresto V., Mennesson B., Traub W. A., Lacasse M. G., 2004, A&A, 418, 675
Ragland S., Traub W. A., Millan-Gabet R., Carleton N. P., Pedretti E., 2003, Proc. SPIE, 4838, 1125
Ragland S. et al., 2008, ApJ, 679, 746
Schild H., Dumm T., Folini D., Nussbaumer H., Schmutz W., 1999, in Cox P., Kessler M., eds, The Universe as Seen by ISO, ESA SP-427. ESA, Noordwijk, p. 397

Downloaded from http://mnras.oxfordjournals.org/ at NASA Goddard Space Flight Ctr on July 1, 2014

Schmidt M. R., Začs L., Mikołajewska J., Hinkle K. H., 2006, A&A, 446, 603
Skopal A., Bode M. F., Lloyd H. M., Tamura S., 1996, A&A, 308, L9
Skopal A., Vaňko M., Pribulla T., Chochol D., Semkov E., Wolf M., Jones A., 2007, Astron. Nachr., 328, 909
Sokoloski J. L., Kenyon S. J., 2003, ApJ, 584, 1021
Soszyński I., 2007, ApJ, 660, 1486
Soszynski I., Udalski A., Kubiak M., Szymanski M. K., Pietrzynski G., Zebrun K., Wyrzykowski O. S. L., Dziembowski W. A., 2004, Acta Astron., 54, 347
Soszynski I. et al., 2007, Acta Astron., 57, 201
Taranova O. G., Iudin B. F., 1988, Ap&SS, 146, 33
Taranova O. G., Shenavrin V. I., 2004, Astron. Rep., 48, 813
Thompson R. R., Creech-Eakman M. J., van Belle G. T., 2002, ApJ, 577, 447
Traub W. A. et al., 2004, Proc. SPIE, 5491, 482
Tuthill P. G., Monnier J. D., Danchi W. C., Wishnow E. H., Haniff C. A., 2000, PASP, 112, 555
van Belle G. T., Ciardi D. R., Thompson R. R., Akeson R. L., Lada E. A., 2001, ApJ, 559, 1155
van Leeuwen F., 2007, Hipparcos, the New Reduction of the New Raw Data, Astrophys. and Space Sci. Library, Vol. 250. Springer, Berlin.
Webster B. L., Allen D. A., 1975, MNRAS, 171, 171
Wood P. R. et al., 1999, in Le Bertre T., Lebre A., Waelkens C., eds, Proc. IAU Symp. 191, Asymptotic Giant Branch Stars. Kluwer, Dordrecht, p. 151
Wood P. R., Olivier E. A., Kawaler S. D., 2004, ApJ, 604, 800
Young J. S. et al., 2000, Proc. SPIE, 4006, 472
Zhao M. et al., 2007, ApJ, 659, 626

This paper has been typeset from a TEX/LATEX file prepared by the author.

Downloaded from http://mnras.oxfordjournals.org/ at NASA Goddard Space Flight Ctr on July 1, 2014